Core/Shell Semiconductor Nanocrystals

Peter Reiss, Myriam Protière, and Liang Li*

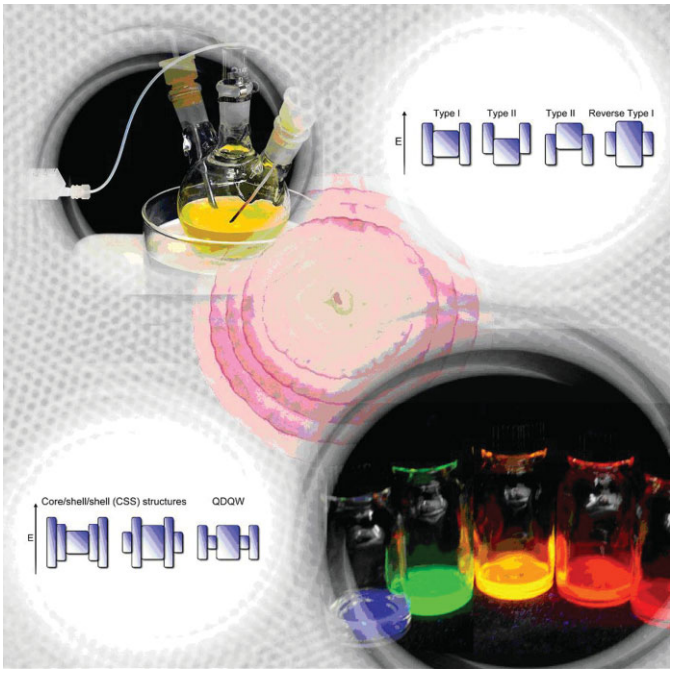

From the Contents

Colloidal core/shell nanocrystals contain at least two semiconductor materials in an onionlike structure. The possibility to tune the basic optical properties of the core nanocrystals, for example, their fluorescence wavelength, quantum yield, and lifetime, by growing an epitaxial-type shell of another semiconductor has fueled significant progress on the chemical synthesis of these systems. In such core/shell nanocrystals, the shell provides a physical barrier between the optically active core and the surrounding medium, thus making the nanocrystals less sensitive to environmental changes, surface chemistry, and photo-oxidation. The shell further provides an efficient passivation of the surface trap states, giving rise to a strongly enhanced fluorescence quantum yield. This effect is a fundamental prerequisite for the use of nanocrystals in applications such as biological labeling and light-emitting devices, which rely on their emission properties. Focusing on recent advances, this Review discusses the fundamental properties and synthesis methods of core/shell and core/multiple shell structures of II–VI, IV–VI, and III–V semiconductors.

NANO MICRO small

1. Introduction

Colloidal semiconductor nanocrystals (NCs), also termed "quantum dots" (QDs), are composed of an inorganic core, made up of between a few hundred and a few thousand atoms, surrounded by an organic outer layer of surfactant molecules (ligands). Their small size results in an observable quantum-confinement effect, defined by an increasing bandgap accompanied by the quantization of the energy levels to discrete values. This effect is accompanied by an exaltation of the coulomb interaction between the charge carriers. For most semiconductors, this observation normally occurs when the particle size is reduced to a few nanometers. These effects significantly modify the processes of intraband and interband relaxation. The size-dependent optical properties of NCs have been the focus of significant research over the past two decades. The nanometric crystal size also results in a very high surface-to-volume ratio. The co-ordination sphere of this high population of surface atoms partially occurs via complex formation with the stabilizing ligands. Nevertheless, a significant fraction of these organically passivated core NCs typically exhibit surface-related trap states acting as fast non-radiative de-excitation channels for photogenerated charge carriers, thereby reducing the fluorescence quantum yield (QY). An important strategy to improve NCs' surface passivation is their overgrowth with a shell of a second semiconductor, resulting in core/shell (CS) systems, the focus of this Review. In this manner, the fluorescence efficiency and stability against photo-oxidation of various types of semiconductor NCs has seen significant improvement. Furthermore, by the appropriate choice of the core and shell materials, it is possible to tune the emission wavelength in a larger spectral window than with both materials alone. After pioneering work in the 1980s and the development of powerful chemical synthesis routes at the end of the 1990s,[1–3] a strongly increasing number of articles have been devoted to CS NCs in the past five years. This work has included two reviews focusing on CdSe based core/shell structures and II–VI core/multishell systems, respectively.[4,5]

The goal of the present review is to discuss the synthesis and basic properties of the different types of core/shell and core/multiple shell NCs of II–VI, IV–VI, and III–V semiconductors reported to date. In addition to a representative overview of the applied chemical synthesis methods, general considerations for the choice of materials and reaction parameters are included, aiming for practical use by the interested reader. In contrast, heterostructures containing core or shell materials other than semiconductors, for example, oxides or metals, are not covered, nor synthesis procedures and fundamental properties of core NCs themselves. The reader is referred to various recent reviews on related topics, namely, on the optical properties of NCs,[6] the synthesis of monodisperse spherical NCs,[7] the fabrication of hybrid NC structures[8] as well as on the application of CS NCs as fluorescent biological labels.[9–11]

2. Classification of Core/Shell Systems

Depending on the bandgaps and the relative position of electronic energy levels of the involved semiconductors, the shell can have different functions in CS NCs. Scheme 1 gives an overview of the band alignment of the bulk materials, which are mostly used in NC synthesis. Three cases can be distinguished, denominated type-I, reverse type-I, and type-II band alignment (cf. Figure 1). In the former, the bandgap of the shell material is larger than that of the core and both electrons and holes are confined in the core. In the second, the bandgap of the shell material is smaller than that of the core and, depending of the thickness of the shell, the holes and electrons are partially or completely confined in the shell. In the latter, either the valence-band edge or the conduction-band edge of the shell material is located in the bandgap of the core. Upon excitation of the NC, the resulting staggered band alignment leads to a spatial separation of the hole and the electron in different regions of the CS structure.

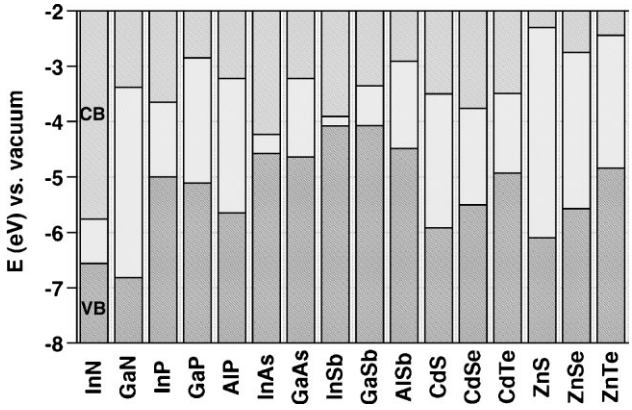

Scheme 1. Electronic energy levels of selected III–V and II–VI semiconductors using the valence-band offsets from Reference [12] (VB: valence band, CB: conduction band).

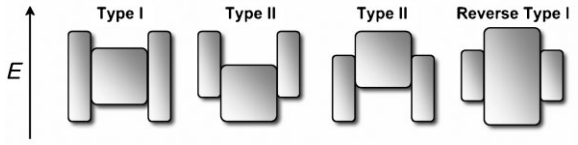

Figure 1. Schematic representation of the energy-level alignment in different core/shell systems realized with semiconductor NCs to date. The upper and lower edges of the rectangles correspond to the positions of the conduction- and valence-band edge of the core (center) and shell materials, respectively.

In type-I CS NCs, the shell is used to passivate the surface of the core with the goal to improve its optical properties. The shell of the NC physically separates the surface of the optically active core from its surrounding medium. Consequently, the sensitivity of the optical properties to changes in the local environment of the NCs' surface, induced, for example, by the

[*] Dr. P. Reiss, Dr. M. Protière, Dr. L. Li
CEA Grenoble, INAC-SPrAM (UMR 5819 CEA-CNRS-UJF) LEMOH
17 rue des Martyrs, 38054 Grenoble cedex 9 (France)
E-mail: peter.reiss@cea.fr

DOI: 10.1002/smll.200800841

presence of oxygen or water molecules, is reduced. With respect to core NCs, CS systems exhibit generally enhanced stability against photodegradation. At the same time, shell growth reduces the number of surface dangling bonds, which can act as trap states for charge carriers and thereby reduce the fluorescence QY. The first published prototype system was CdSe/ZnS. The ZnS shell significantly improves the fluorescence QY and stability against photobleaching. Shell growth is accompanied by a *small* red shift (5–10 nm) of the excitonic peak in the UV/Vis absorption spectrum and the photoluminescence (PL) wavelength. This observation is attributed to a partial leakage of the exciton into the shell material.

In reverse type-I systems, a material with narrower bandgap is overgrown onto the core with wider bandgap. Charge carriers are at least partially delocalized in the shell and the emission wavelength can be tuned by the shell's thickness. Generally, a significant red-shift of the bandgap with the shell thickness is observed. The most extensively analyzed systems of this type are CdS/HgS,[13] CdS/CdSe,[14] and ZnSe/CdSe.[15] The resistance against photobleaching and the fluorescence QY of these systems can be improved by the growth of a second shell of a larger-bandgap semiconductor on the core/shell NCs.[14]

In type-II systems, shell growth aims at a *significant* red-shift of the emission wavelength of the NCs. The staggered band alignment leads to a smaller effective bandgap than each one of the constituting core and shell materials. The interest of these systems is the possibility to manipulate the shell thickness and thereby tune the emission color towards spectral ranges, which are difficult to attain with other materials. Type-II NCs have been developed in particular for near-infrared emission, using for example CdTe/CdSe or CdSe/ZnTe. In contrast to type-I systems, the PL decay times are strongly prolonged in type-II NCs due to the lower overlap of the electron and hole wavefunctions. As one of the charge carriers (electron or hole) is located in the shell, an overgrowth of type-II CS NCs with an outer shell of an appropriate material can be used in the same way as in type-I systems to improve the fluorescence QY and photostability. Both type-I and type-II CS NCs have been the object of recent theoretical studies, giving further insight into the electronic structure of these systems.[16–18]

3. General considerations for the design of core/shell systems

3.1. Choice of the Shell Material

A general requirement for the synthesis of CS NCs with satisfactory optical properties is *epitaxial-type shell growth*. Therefore an *appropriate band alignment* is not the sole criterion for the choice of materials but rather the core and shell materials should *crystallize in the same structure and exhibit a small lattice mismatch*. In the opposite case, the growth of the shell results in strain and the formation of defect states at the core/shell interface or within the shell. These can act as trap states for photogenerated charge carriers and diminish the fluorescence QY.[19] Table 1 lists the materials' parameters of selected semiconductors.

Dr. Peter Reiss obtained his Ph.D. in inorganic chemistry from the University of Karslruhe (Germany) in 2000. The same year he was appointed by the Institute of Nanosciences and Cryogenics (INAC) of the Atomic Energy Commission (CEA) Grenoble, France, where he is presently the nanomaterials group leader. His scientific interests involve the synthesis of semiconductor nanocrystals and magnetic nanoparticles, their applications in biological labeling, optoelectronics, and data storage as well as the preparation and processing of their composites with electroactive polymers. Dr. Reiss has published over 30 scientific papers and holds 5 patents. He acts as an Assistant Editor for *Nanoscale Research Letters* and co-organizes the biennial conference "Nanoscience with Nanocrystals".

Dr. Myriam Protière is a post-doctoral researcher at CEA-INAC Grenoble, France. She received her degree in chemistry and chemical engineering from ENSIACET Toulouse in 2004, and her Ph.D. in chemistry from Joseph Fourier University, Grenoble, in 2007. During her Ph.D. she developed the synthesis of various types of fluorescent core/shell semiconductor nanocrystals and the scale-up of this synthesis. She currently studies the structure and reactivity of natural organic matter by electron paramagnetic resonance.

Dr. Liang Li is currently a post-doctoral researcher at CEA-INAC Grenoble, France. He obtained his Ph.D. degree in applied chemistry from Shanghai JiaoTong University in 2006, where he worked on the aqueous synthesis of nanocrystals for bio-applications. His current research focuses on the chemical synthesis of cadmium-free semiconductor nanocrystals of core and core/shell-type nanocrystals, such as III–V quantum dots and I–III–VI ternary nanocrystals.

3.2. Precursors for Shell Growth

Appropriate precursors for shell growth should fulfill the criteria of high reactivity and selectivity (no side reactions). For practical reasons, and in particular if the scale-up of the production process is sought, additional properties of the precursors come into play. Pyrophoric and/or highly toxic compounds require special precautions for their manipulation, especially if used in large quantities. An example is the synthesis of zinc sulfide, one of the most important shell materials used for overcoating numerous II–VI and III–V semiconductor NCs. Initially, this synthesis was made with

NANO MICRO small

Table 1. Material parameters of selected bulk semiconductors.[20,21]

Material	Structure [300K]	Type	E_{gap} [eV]	Lattice parameter [Å]	Density [kg m^{-3}]
ZnS	Zinc blende	II–VI	3.61	5.41	4090
ZnSe	Zinc blende	II–VI	2.69	5.668	5266
ZnTe	Zinc blende	II–VI	2.39	6.104	5636
CdS	Wurtzite	II–VI	2.49	4.136/6.714	4820
CdSe	Wurtzite	II–VI	1.74	4.3/7.01	5810
CdTe	Zinc blende	II–VI	1.43	6.482	5870
GaN	Wurtzite	III–V	3.44	3.188/5.185	6095
GaP	Zinc-blende	III–V	2.27	5.45	4138
GaAs	Zinc blende	III–V	1.42	5.653	5318
GaSb	Zinc blende	III–V	0.75	6.096	5614
InN	Wurtzite	III–V	0.8	3.545/5.703	6810
InP	Zinc blende	III–V	1.35	5.869	4787
InAs	Zinc blende	III–V	0.35	6.058	5667
InSb	Zinc blende	III–V	0.23	6.479	5774
PbS	Rocksalt	IV–VI	0.41	5.936	7597
PbSe	Rocksalt	IV–VI	0.28	6.117	8260
PbTe	Rocksalt	IV–VI	0.31	6.462	8219

diethylzinc (pyrophoric) and hexamethyldisilathiane (toxic). Even though widely used in laboratory-scale syntheses, these compounds are not suitable for large-scale production of ZnS-overcoated NCs. Therefore, a number of alternative precursors have recently been proposed. These compounds include zinc carboxylates and elemental sulfur, as well as monomolecular precursors such as zinc xanthates or zinc dithiocarbamates. Further criteria to be taken into account concern the environmental risks related to the use of the precursors and their degradation products, their cost, and their commercial availability. As it is rather difficult to satisfy all of these factors, the development of shell-synthesis methods is an active area of research.

3.3. Control of the Shell Thickness

The control of the shell thickness is a delicate point in the fabrication of CS NCs and deserves special attention. If the shell is too thin, the passivation of the core NCs is inefficient, resulting in reduced photostability. In the opposite case, the optical properties of the resulting CS NCs generally deteriorate as a consequence of strain induced by the lattice mismatch of the core and shell materials, accompanied by the generation of defect states.

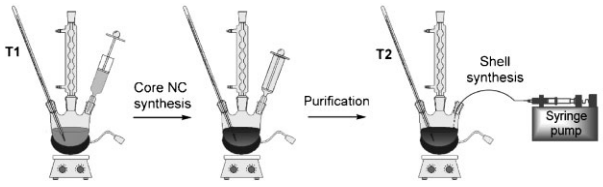

Figure 2. Two–step synthesis of core/shell nanocrystals.

CS systems are mostly fabricated in a *two-step* procedure: initial synthesis of core NCs, followed by a purification step, and the subsequent shell growth reaction. During this final step, a small number of monolayers (typically 1–5) of the shell material are deposited on the cores (Figure 2). In order to prevent nucleation of the shell material and uncontrolled ripening of the core NCs, the temperature $T2$ for the shell growth is generally lower than $T1$ used for the core NC synthesis. Furthermore, the shell precursors are slowly added, for example, by means of a syringe pump. A major advantage over a so-called *one-pot* approach without an intermediate purification step is the fact that unreacted precursors or side products can be eliminated before the shell growth. The core NCs are purified by precipitation and redispersion cycles, and finally dissolved in the solvent used for the shell growth. In order to calculate the required amount of shell precursor to obtain the desired shell thickness, it is necessary to know the concentration of the core NCs. This information can be obtained by carefully drying the NC sample and weighing and determining its composition by elemental analysis using atomic absorption spectroscopy. Correlation of the data with the NCs' size, obtained by transmission electron microscopy (TEM), allows for the calculation of the molar quantity of NCs in the investigated sample. As the NC size is directly related to the excitonic peak in the UV/Vis absorption spectrum, the size-dependent molar extinction coefficient ε can be determined at the same time. There are several materials for which the correlation between the NC size and ε has been tabulated in the literature, such as CdSe, CdS, CdTe,[22] and InP.[23] Table 2 lists empirical mathematical functions describing, in good approximation, the size-dependent optical properties of the cited II–VI semiconductor NCs.

Table 2. Empirical functions correlating the size of CdSe, CdS, CdTe, and InP NCs with the position of the excitonic peak in their UV/Vis absorption spectra and with the molar extinction coefficient D and λ in nm; ε in L mol^{-1} cm^{-1}).[22,24]

Material	Correlation diameter D/excitonic peak λ
CdSe	$D = (1.6122 \times 10^{-9})\lambda^4 - (2.6575 \times 10^{-6})\lambda^3 + (1.6242 \times 10^{-3})\lambda^2 - (0.4277)\lambda + (41.57)$
CdTe	$D = (9.8127 \times 10^{-7})\lambda^3 - (1.7147 \times 10^{-3})\lambda^2 + (1.0064)\lambda - (194.84)$
CdS	$D = (-6.6521 \times 10^{-8})\lambda^3 + (1.9557 \times 10^{-4})\lambda^2 - (9.2352 \times 10^{-2})\lambda + (13.29)$
InP	$D = (-3.7707 \times 10^{-12})\lambda^5 + (1.0262 \times 10^{-8})\lambda^4 - (1.0781 \times 10^{-5})\lambda^3 + (5.4550 \times 10^{-3})\lambda^2 - (1.3122)\lambda + 119.9$
Material	**Correlation ε/excitonic peak λ**
CdSe	$\varepsilon = 5857(D)^{2.65}$
CdTe	$\varepsilon = 10043(D)^{2.12}$
CdS	$\varepsilon = 21536(D)^{2.3}$
InP	$\varepsilon = 3046.1(D)^3 - 76532(D)^2 + (5.5137 \times 10^5)(D) - (8.9839 \times 10^5)$

As a consequence, the concentration of a dispersion containing NCs of these materials can easily be determined by UV/Vis spectroscopy using the Beer–Lambert law:

$$A = \varepsilon * c * l \quad (1)$$

where A, ε, c, and l are absorbance, molar absorbtivity (L mol^{-1} cm^{-1}), NC concentration (mol L^{-1}), and path length of the cuvette in which the sample is contained (cm), respectively.

Despite the fact that the calculation is based on two empirical formulae, both of which contain a certain error level,[22] the presented procedure significantly simplifies the determination of the molar concentration of NCs in a given dispersion. The data of a single absorption spectrum is exploited, whereas otherwise the sample weight would have to be determined after careful drying. Another advantage of the described method is that it is entirely based on the properties of the inorganic core of the NCs and not on the organic surfactant layer at the surface, giving more accurate results.

With the knowledge of the NCs' size and molar quantity, the amount of precursor for the growth of a shell of material CD, having the desired thickness of x monolayers, on the surface of core NCs AB can be calculated, using the bulk crystal parameters of the shell material, as follows:

$$V_{CD}(ML_x) = 4/3 * \pi * ((r_{AB} + x * d)^3 - r_{AB}^3) \quad (2)$$

$$n_{CD}(ML_x) = \rho_{CD} * V_{CD}(ML_x) * 10^{-27}/m_{CD} \quad (3)$$

$$n_{CD} = n_{AB} * n_{CD}(ML_x) \quad (4)$$

where $V_{CD}(ML_x)$ is the volume of the shell comprising x monolayers (nm^3), r_{AB} is the radius of the core NCs (nm), d is the thickness of one shell monolayer (nm), $n_{CD}(ML_x)$ is the number of CD monomer units per NC contained in x shell monolayers (dimensionless), ρ_{CD} is the density of the bulk shell material (kg m^{-3}), m_{CD} is the mass of a shell monomer unit (kg), n_{CD} is the molar quantity of precursor CD needed for the growth of x monolayers (mmol), and n_{AB} is the molar quantity of core NCs used for the synthesis of the CS system (mmol).

The term "monomer" signifies, in accordance with common practice, the hypothetical smallest subunit of the shell material consisting of one cation and one anion. Equations (2–4) do not contain corrections for the treatment of NCs of shapes differing from perfect spheres, nor do they take account of the deviation of the materials' constants at the NC surface from those of the bulk semiconductors. Furthermore, a quantitative reaction is assumed, during which the total amount of the injected shell precursors are homogeneously deposited on the existing core NCs. Nevertheless, the validity of the described approach has unambiguously been demonstrated in an approach for shell growth derived from chemical-bath deposition techniques, the so-called SILAR (successive ion layer adsorption and reaction) method.[25] It is based on the formation of one monolayer at a time by alternating the injections of cationic and anionic precursors

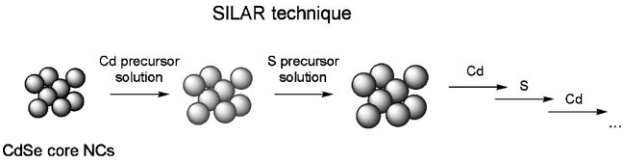

Figure 3. Shell synthesis using the SILAR method, schematically illustrated for the CdSe/CdS core/shell system.

and has initially been applied for the synthesis of CdSe/CdS CS NCs (Figure 3). Monodispersity of the samples was maintained for CdS shell thicknesses up to 5 monolayers on 3.5-nm-core CdSe NCs, as reflected by the narrow PL line widths obtained in the range of 23–26 nm (full width at half-maximum, FWHM).

A new strategy aiming at the simplification of the core/shell synthesis within a single step deserves mentioning here.[26] In this example, CdSe/ZnS NCs of a pseudo core/shell structure with a composition gradient are obtained upon injection of the chalcogenide precursors into a hot mixture of the metal precursors and stabilizers. Due to the difference in reactivity of the used precursors, first the CdSe core forms, and subsequently the overgrowth with the graded $Cd_{1-x}Zn_xS$ shell takes place, leading to monodisperse CS NCs.

3.4. Characterization of CS Systems

Most of the basic characterization techniques for CS systems are also applied to investigate core NCs, such as UV/Vis and PL spectroscopy, powder X-ray diffraction or transmission electron microscopy (TEM). In the case of CS NCs, however, several experimental difficulties may arise in proving successful shell growth. Optical properties, generally extremely sensitive to NC surface modification, can only give indirect information about the possible overcoating with a shell and therefore spectroscopic analyses (UV/Vis, PL) must be completed by structural studies. The increase of the NCs' diameter revealed by TEM or -esolution (HR) TEM is considered to be the most direct proof of successful shell growth. Nevertheless, an accurate determination of the size difference before and after addition of the shell can be severely limited or even impossible by TEM depending on the materials used, the size and size distribution of the core NCs, as well as the shell thickness. Advanced microscopy techniques including scanning transmission electron microscopy (STEM) coupled with electron energy loss spectroscopy (EELS) or with energy-dispersive X-ray spectroscopy (EDX) can give valuable insight into the obtained CS structures. As an example, the former technique has been applied to characterize CdSe/ZnS CS NCs, revealing a highly anisotropic distribution of the shell material around the core NCs.[27]

Among other, more sophisticated characterization methods for CS NCs, X-ray photoelectron spectroscopy (XPS) should be cited. This method is a powerful tool to simultaneously investigate the core/shell interface, the shell thickness, and even the NCs' surface properties, such as the binding modes of surface ligands.[28–31] Related techniques such as extended X-ray absorption fine structure (EXAFS)

NANO MICRO small

have been used to a lesser extent for the characterization of the nature and binding modes of NC suface ligands.[32,33] Several reports on the use of Raman spectroscopy to investigate the phonon spectra associated with CS systems have appeared in recent literature, highlighting the utility of this technique to assess the quality of the prepared samples.[34–36] Finally, as the lifetime of the excited state is dependent on the probability of radiative recombination, which itself is a function of the band structure in CS NCs, time-resolved PL spectroscopy is an appropriate tool for the characterization of type-II systems or type-I/type-II transitions.[37,38]

4. Synthesis of Type-I Core/Shell Nanocrystals

As already mentioned in Sectionr 2, type-I systems are generally synthesized with the goal to increase the fluorescence QY and stability against photobleaching by improving NC surface passivation. Unless otherwise stated, the shell precursors are slowly injected into a dispersion of the purified core NCs.

4.1. II–VI SC NCs

The most studied CS structure to date is CdSe/ZnS, as evidenced by the number of publications dealing with this system. Its synthesis was first described by Hines and Guyot-Sionnest, who overcoated 3-nm CdSe NCs with 1–2 monolayers of ZnS, resulting in a QY of 50%.[1] ZnS shell growth has been achieved by the injection of a mixture of the organometallic precursors diethylzinc and hexamethyldisilathiane, also known as bis(trimethylsilyl)sulfide, $S(TMS)_2$, at high temperature (300 °C). Using shell growth temperatures of 140–220 °C (depending on the core size), a whole size series of CdSe/ZnS NCs and their in-depth characterization was reported shortly afterwards by Bawendi's group.[2] A similar approach has later been applied for the ZnS capping of CdSe nanorods with lengths up to 30 nm.[39] The addition of hexadecylamine (HDA) to the traditionally used solvent system trioctylphosphine oxide/trioctylphosphine (TOPO/TOP) led to a better control of the growth kinetics during both the CdSe core and ZnS shell synthesis, resulting in a lower size distribution and QYs on the order of 60%.[40] Recently, extremely small CdSe/ZnS CS NCs have been synthesized by Kudera et al., making the blue spectral region accessible with this system.[41] The synthetic approach was based on the sequential growth of CdSe "magic-sized" clusters in a mixture of trioctylphosphine, dodecylamine, and nonanoic acid at temperatures of 80 °C and their subsequent coating with ZnS. Another procedure to access this spectral region was suggested by Jun and Jang:[42] the ZnS overgrowth process was performed at 300 °C using precursors (zinc acetate and octanethiol) of relatively low reactivity; the shell material then diffused into the core, resulting in a significant hypsochromic shift of the emission wavelength. The obtained NCs emit at 470 nm with a QY of 60%. Shell growth on wurtzite CdSe core NCs, generally obtained with the hot-injection method, is kinetically driven along the *c*-axis.[43] With the goal to enhance the uniformity of shell growth, zinc blende CdSe NCs have been used for overgrowth with ZnS by Lim et al., as this structure has a more isotropic distribution of facets than the wurtzite model.[44] Multimodal CS NCs appropriate for both optical and magnetic resonance imaging techniques have been obtained by doping of the ZnS shell with manganese ions in the range of 0.6–6.2%.[45] In this case, the growth of the $Zn_{1-x}Mn_xS$ shells of 1 to 6 monolayer thickness was achieved by injection of a mixture of diethylzinc, dimethylmanganese, and H_2S gas to a dispersion of the CdSe core NCs at 170 °C.

A CdSe-based system exhibiting a different band alignment is CdSe/CdS (cf. Scheme 1). In this common cation heterostructure, a large band offset for the holes is combined with a relatively small one for the electrons. Epitaxial growth is favored by the comparably small lattice mismatch of around 4% between the core and shell material. Peng et al. reported the synthesis and detailed characterization of a series of CdSe/CdS NCs with core diameters ranging from 2.3 to 3.9 nm and QYs above 50%.[3] In contrast to the CdSe/ZnS system, exhibiting a rather small bathochromic shift (5–10 nm) of the excitonic and PL peak upon shell growth, these features here are continuously shifting throughout the shell growth, thereby indicating a delocalization of the electron over the entire CS structure. While in this early report organometallic precursors (dimethylcadmium, bis(trimethylsilyl)sulfide) had been used, the synthesis of this CS system was more recently carried out using air-stable precursors, *i.e.* cadmium oleate and elemental sulfur dissolved in octadecene (Figure 4).[25] The SILAR method has recently been extended to the synthesis of "giant" CdSe/CdS NCs with a shell thickness as high as approximately 6 nm (19 CdS monolayers) and to CdSe/CdS/$Cd_{1-x}Zn_xS$/ZnS

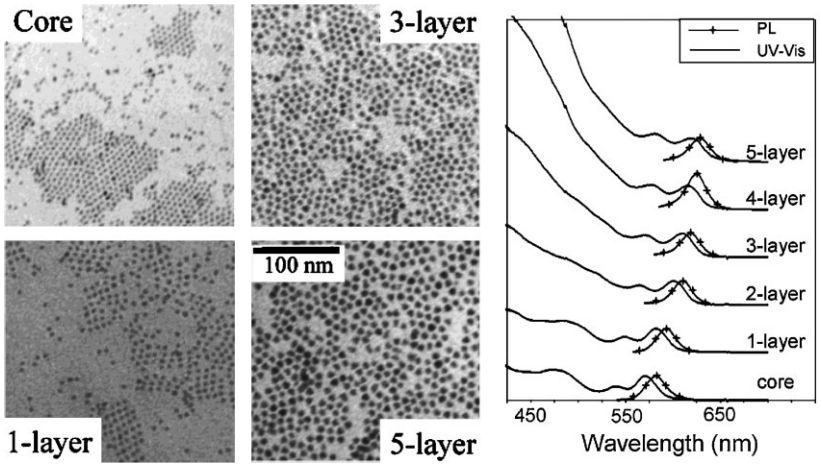

Figure 4. Left panel: TEM images of CdSe NCs depicting the increase in diameter upon growth of several monolayers of a CdS shell by means of the SILAR technique. Right panel: UV/Vis and PL spectra of samples with different shell thicknesses. Reprinted with permission from Reference [25]. Copyright 2001, American Chemical Society.

NCs comprising a graded shell.[46,47] The goal of these syntheses was to render the NCs' optical properties independent of their surface chemistry and environment by a thick inorganic shell. The produced samples exhibited a very high stability against photobleaching and, in a significant fraction of the analyzed individual NCs, the blinking phenomenon was suppressed. O'Brien and co-workers extended their work on monomolecular precursors on CdSe/CdS NCs using bis(hexyl (methyl)dithiocarbamato) and bis(hexyl(methyl) diselenocarbamato) cadmium compounds for the core NC and shell growth, respectively.[48,49] Another modification of the original protocol[3] concerned the omission of the intermediate purification step of the core NCs, defining growth of the CS structure in a so-called *one-pot* synthesis and yielding NCs with QYs in the range of 50–85%.[50] In addition, alternative precursors for the shell growth have been proposed in the same article, namely, in situ generated H_2S gas and cadmium acetate. The preparation of particularly small CdSe/CdS CS NCs with core sizes in the range of 1.2–1.5 nm, emitting in the range of 445 to 517 nm with QYs of 60–80%, has been described by Pan et al. (cf. Figure 5).[51] Both core and shell syntheses were carried out at 180/140 °C in an autoclave using cadmium myristate and selenourea/thiourea as precursors, oleic acid as a stabilizer, and a toluene/water two-phase solvent. Further reports focus on the cost reduction by exchanging solvents such as TOPO or octadecene by heat-transfer fluids[52] or by carrying out the whole synthesis in aqueous media.[53] In the latter case, CdSe was prepared from cadmium nitrate and 1,1-dimethylselenourea precursors under illumination with a pulsed Nd:YAG laser at 532 nm, followed by CdS shell growth using thioacetamide as the S source. The PL QY of the obtained NCs was increased from a few percent to 60% by an additional UV irradiation step (24 h with a 100 W Hg-Xe lamp).

CdSe/ZnSe is a CS system exhibiting, in contrast to CdSe/CdS, efficient confinement of the electrons in the NC core due to the large conduction-band offset. On the other hand, only a relatively small barrier exists for the holes in this system. Although the lattice mismatch is larger than in CdSe/CdS (6.3 versus 3.9%), the common anion structure is particularly favorable for epitaxial-type shell growth. However, initially reported CdSe/ZnSe NCs exhibited rather low values of the PL QY (<1%).[54] Subsequently, a modified synthesis method has been introduced using the air-stable precursor zinc stearate rather than diethylzinc as the zinc source in combination with selenium dissolved in trioctylphosphine (TOPSe) as the Se source.[55,56] The CS NCs obtained with this method exhibited QYs ranging from 60–85% and narrow emission line widths. Lee et al. studied the effect of lattice distortion in the CdSe/ZnSe CS system on the optical spectra by varying the concentration of the ZnSe precursor solution used for the shell growth,[57] as well as the ripening kinetics upon thermal annealing.[58]

Figure 5. Photograph of CdSe/CdS CS NCs with core sizes ranging from 1.2 to 1.5 nm, exhibiting PL Q.Y.s of 60–80% (under room light). Reproduced with permission from Reference [51].

Both CdSe/CdS and CdSe/ZnSe heterostructures exhibit high fluorescence QYs and can have specific interests due to the "accessibility" of the weakly confined electrons or holes, respectively. On the other hand, if purely high stability of the optical properties against photodegradation and chemical inertness of the shell material are researched, zinc sulfide is the shell material of choice. Although it is, in principle, possible to obtain green, or even blue, emission with CdSe NCs of small size, their capping with ZnS has only very recently been achieved.[41] As a matter of fact, an analysis of the present state-of-the-art methods suggests that for a large variety of materials, the preparation of CS NCs of low size dispersion and satisfying optical properties is facilitated when core NCs with diameters in the range of approximately 2.5 and 5 nm are used. Consequently, the synthesis of core NCs other than those of CdSe has been developed in order to better cover the green/blue/UV and the near-infrared spectral regions. In this context, an interesting alternative to the tuning of the emission color with size is the formation of alloy structures, allowing for the color variation by changing the composition of the NCs. Examples are $Cd_{1-x}Zn_xSe$ NCs, the bandgap of which can be varied by changing x between the values of pure CdSe and pure ZnSe NCs of the same size. This system is particularly interesting for the fabrication of efficient green emitters for use in display applications. To do so, the alloy core NCs have been overgrown with a ZnS shell either using the established diethylzinc/bis(trimethylsilyl)sulfide method[59] or, more recently, by means of the air-stable monomolecular precursor zinc diethylxanthate.[60] In the latter case, after growth of three ZnS monolayers, the obtained CS NCs emitted at 530 nm with a line width of 35 nm (FWHM) and a QY of 65%.

Emission wavelengths in the blue and near-UV spectral region have been obtained by using larger-bandgap core materials, in particular CdS and ZnSe. It is noteworthy that CdS, "activated" by a shell of cadmium hydroxide, is historically the first example of colloidal CS NCs reported in the literature.[61] After treatment of 4–6-nm CdS core NCs with NaOH and $Cd(ClO_4)_2$ in aqueous solution, samples with a PL QY around 50% and narrow emission line widths were obtained. The emission wavelength range was extended to the blue range when CdS-ZnS co-colloids were activated in the same fashion. In organic media, CdS NCs have later been overgrown with a ZnS shell using the classical organometallic approach with dimethylcadmium and $S(TMS)_2$ as precursors, yielding an emission in the range of 460–480 nm (FWHM 24–28 nm) with QYs of 20–30%.[62] Recently, these reagents were replaced by a combination of the air-stable monomolecular precursors zinc ethylxanthate and zinc stearate, resulting in monodisperse CdS/ZnS CS NCs emitting in the range of 440–480 nm (15–18 nm FWHM) with QYs of 35–45% (Figure 6).[63]

The CdS core NCs have further been used as a host matrix for Mn dopant ions in CdS:Mn/ZnS CS systems, either

small NANO MICRO

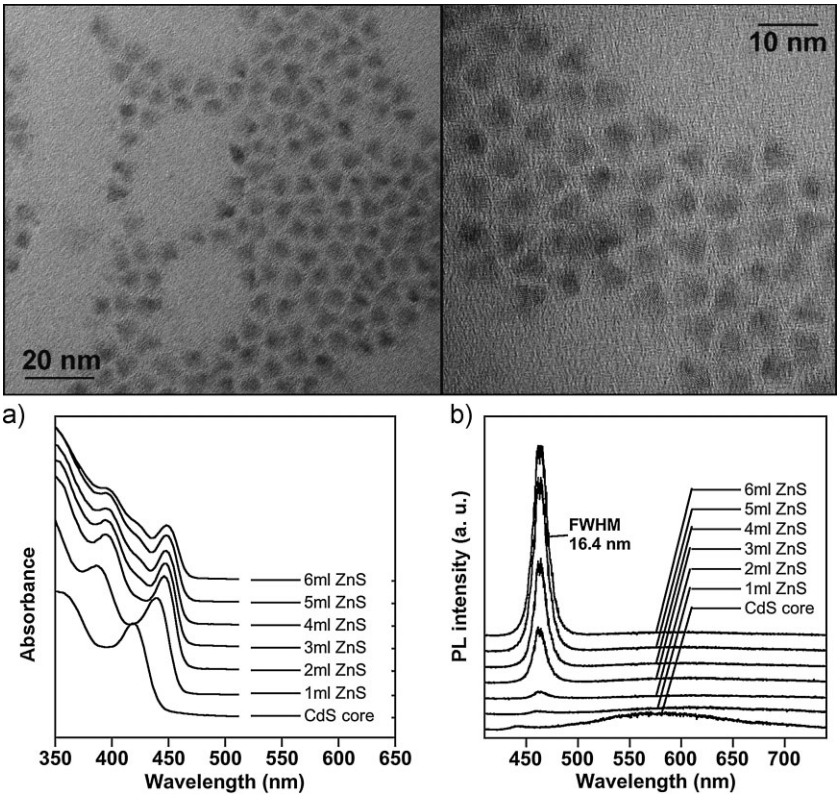

Figure 6. Top: TEM images at different magnifications of CdS/ZnS NCs. [63] Bottom: a) UV/Vis absorption spectra; b) PL spectra recorded during the addition of 6 mL of the ZnS precursor solution corresponding to the growth of a 5-monolayer-thick ZnS shell on 4-nm CdS core NCs.

prepared by the organometallic route or by the reverse micelle technique.[64,65] ZnSe has equally been overcoated by ZnS using organometallic precursors, leading to emission wavelengths in the range of 400 nm, PL line widths of 20 nm and QYs on the order of 15%.[66] A newer approach based on the use of alternative precursors such as ZnO and TOPSe for the core NCs and zinc laurate and TOPS for the shell growth and carried out at 180 °C in HDA yielded ZnSe/ZnS CS NCs with QYs up to 30%.[67]

Cadmium telluride, exhibiting a smaller bulk bandgap than cadmium selenide (1.5 versus 1.75 eV at 300 K) is, in principle, a good candidate for the fabrication of red- or near-infrared-emitting quantum dots. Although the reported synthesis methods for CdSe could generally be adapted for CdTe, comparably little work exists concerning the preparation of related CS systems in organic solvents such as, for example, CdTe/ZnS.[68] At the origin of this trend is the fact that most of the appropriate shell materials resulting in a type-I band alignment exhibit a large lattice mismatch with respect to CdTe. However, the preparation of thiol-stabilized CdTe NCs in aqueous media, pioneered by Weller's group, has seen a huge success.[69] CdS is the shell material of choice in CS systems derived from the aqueous synthetic approach as it can be produced in situ by transformation of the surface thiols. Initially, highly luminescent NCs (QY up to 85%) were prepared through the illumination-induced release of sulfide ions from the thioglycolic acid stabilizing ligands. These released ions reacted with surface Cd atoms to form a CdS shell.[70] More recently, in similar studies, the in situ formation of the CdS shell was accelerated by means of microwave and ultrasonic irradiation, respectively.[71,72]

A further shift to the near-infrared spectral region, and in particular towards 1.3 and 1.55 μm used in fiber-optics-based telecommunication, has been achieved by using HgTe/CdSCS NCs.[73] The synthesis of this system comprised the preparation of thioglycerol-stabilized HgTe core NCs, prepared in aqueous media in a similar manner as CdTe. For the CdS overcoating, H_2S gas and cadmium perchlorate were used.

4.2. III–V Semiconductor NCs

Literature on III–V semiconductor based CS systems is far less extensive than in the case of II–VI compounds, as a consequence of the lack of robust synthesis methods for most core NCs of this family. However, due to the low acceptability of cadmium- and lead-containing materials for technological applications, increasing research effort has been noted in recent years. Indium phosphide is the most studied compound, as the emission of InP NCs can be tuned throughout the visible and near-infrared range by changing their size. However, as-prepared InP NCs exhibit rather poor optical properties as compared to CdSe. The PL line width is significantly broader, on the order of 50–100 nm (FWHM), and band-edge emission peaks related to defect-state emission occur in the spectrum. Furthermore, the QY is low, typically less than 1%.[74–76] The groups of Mićić and subsequently Talapin described an efficient way to increase the QY of InP NCs to values of 30–40% by photoassisted etching of their surface with HF.[77,78] This process resulted in the removal of surface phosphorous atoms lying at the origin of trap states, which provided non-radiative recombination pathways. Concerning InP-based CS systems, Haubold et al. used organometallic precursors to grow a ZnS shell on InP and observed a subsequent increase of the QY to 15% after three days and 23% after three weeks during a slow, room-temperature process.[79] In order to adjust the lattice parameters of the core and shell materials and to reduce strain-induced defects, Mićić and co-workers developed a $CdZnSe_2$ shell leading to a fluorescence QY of 5–10%.[80]

In 2007, two further articles appeared describing new procedures for the overgrowth of InP NCs with ZnS. Xie et al. synthesized high-quality InP core NCs at comparably low temperature (around 190 °C) by adding a low-boiling-point primary alkylamine to the reaction mixture in order to activate the indium carboxylate precursor.[82] Upon ZnS shell growth using sulfur and zinc stearate in ODE, a fluorescence QY of up to 40% is obtained. Li et al. reported a novel, low-cost method

for the preparation of InP core NCs based on the in situ generation of phosphine gas from a metal phosphide (calcium phosphide) precursor. In addition, this approach allowed for the synthesis of large-sized particles without sacrificing the size distribution.[83] Subsequent capping with a ZnS shell was achieved by means of the monomolecular precursor zinc ethylxanthate and led to fluorescence QYs in the range of 10–22%, depending on the emission wavelength. Nann and co-workers published the synthesis of InP/ZnS NCs with QYs up to 60%, obtained by improving the surface quality of the core NCs through the addition of zinc undecylenate and hexadecylamine to the reaction mixture and subsequent ZnS shell growth using zinc diethyldithiocarbamate (Figure 7).[81] More recently, the single-step synthesis of InP/ZnS CS NCs without precursor injection has been reported.[84] In this approach, based on the different reactivity of the applied core (indium myristate, $P(TMS)_3$) and shell (zinc stearate, 1-dodecanethiol) precursors, all reagents are mixed at room temperature and subsequently heated to 250–300 °C. The samples obtained with this method exhibited an emission range of 480–590 nm and fluorescence QYs of 50–70%. These developments evidence the recent progress in the synthesis of InP/ZnS CS NCs exhibiting optical properties of similar quality as those obtained with CdSe-based systems. Nevertheless, a detailed structural characterization and precise determination of the shell thickness are lacking in most reports. The latter is obviously complicated by the increased size distribution of the core InP NCs as compared to their II–VI semiconductor counterparts.

Using InAs core NCs, Cao and Banin prepared several near-infrared-emitting CS structures with InP, GaAs, CdSe, ZnSe, and ZnS shells via the high-temperature pyrolysis of organometallic precursors in TOPO.[85,86] The obtained fluorescence QYs depended on the shell material. In the case of InP, PL quenching was observed, whereas ZnS led to a QY of 8%. For CdSe and ZnSe, an enhancement up to 20% was detected. More recently, the synthesis of a series of small InAs/ZnSe CS NCs has been described, aiming at emission wavelengths in the range of 700–900 nm.[87] This spectral region is especially well adapted for in vivo biological imaging due to the reduced light scattering by the tissue. The obtained NCs exhibited a QY of 6–9% after transfer to the aqueous phase and were successfully applied for the in vivo imaging of lymph nodes.

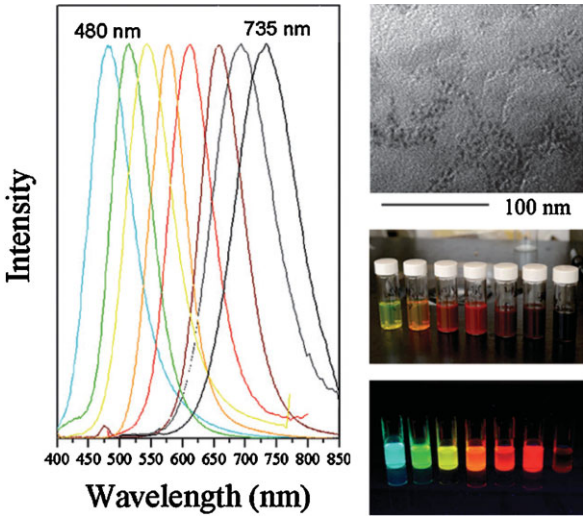

Figure 7. Left: PL spectra of different sized InP/ZnS CS NCs. Right top: TEM image (mean particle diameter: 4.5 nm); middle: different sized samples under room light; bottom: under UV light. Reprinted with permission from Reference [81]. Copyright 2008, Royal Society of Chemistry.

4.3. IV–VI Semiconductor NCs

In contrast to the discussed II–VI and III–V semiconductors, exhibiting either the hexagonal wurtzite or the cubic zinc blende crystal structure, the IV–VI family is characterized by the rocksalt structure (cf. Table 1). Only lead-based NCs (PbS, PbSe) have been studied in the form of CS systems. The bulk bandgaps of these compounds are comparably small and they are, therefore, good candidates for the design of near-infrared emitters. Lifshitz and coworkers reported the synthesis of PbSe/PbS and $PbSe/PbSe_xS_{1-x}$ CS NCs emitting in the range of 1–2 μm with QYs of 40–50% and 65%, respectively, through the use of lead(II)acetate, TOPSe and TOPS as precursors, oleic acid as stabilizer, and diphenylether as the solvent (Figure 8).[88–90] The SILAR method, previously mentioned in the case of CdSe/CdS, has recently been applied for the synthesis of PbSe/PbS NCs.[91] Talapin et al. recently synthesized PbSe/PbS CS spheres and nanowires, tailoring the morphology of the core NCs by addition of co-surfactants (e.g., alkylamines, alkylphosphonic acids) and using lead acetate in octyl ether and sulfur in ODE as the shell precursors.[92] To the contrary of cited reports, Stouwdam et al. did not observe any stability enhancement against photo-oxidation of the PbSe/PbS CS system as compared to PbSe NCs capped by organic surfactants.[93] To this end, Hollingsworth and co-workers developed PbSe/CdSe CS NCs by the exchange of surface lead ions by cadmium.[94] A strongly improved stability of the optical properties was observed,

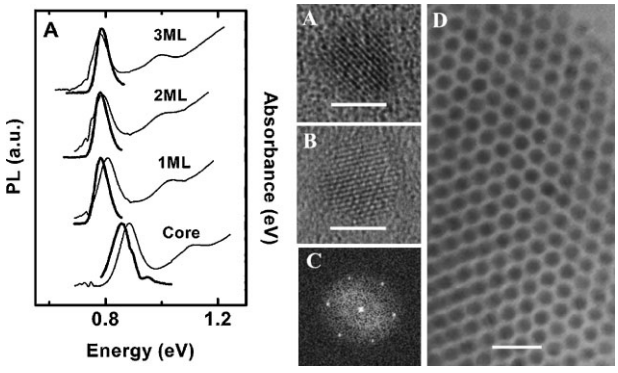

Figure 8. Left panel: Evolution of the UV/Vis absorption and PL spectra of 4.9-nm PbSe core NCs during the growth of indicated thickness. Right panel: A) HRTEM image of a PbSe/PbS CS NC comprising a 4.8-nm core and a 1.2-nm shell; B) HRTEM image of a $PbSe/PbSe_{0.5}S_{0.5}$ core/alloyed shell NC; C) FFT image of the particle in image (A); D) TEM image of self-assembled 6.7-nm core/alloyed shell NCs. The scale bars are 5 nm in (A) and (B), and 20 nm in (D). Reprinted with permission from Reference [89]. Copyright 2006, American Chemical Society.

NANO MICRO small

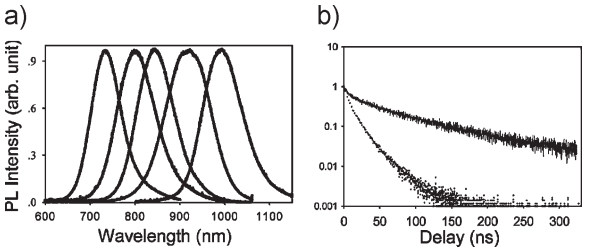

Figure 9. a) Normalized PL spectra of CdTe/CdSe CS NCs having a core/shell radii of 1.6/1.9 nm, 1.6/3.2 nm, 3.2/1.1 nm, 3.2/2.4 nm, 5.6/1.9 nm (from left to right, respectively). b) Normalized PL decays of 3.2/1.1-nm CdTe/CdSe CS NCs and of the corresponding 3.2-nm CdTe core NCs (dotted line). Reprinted with permission from Reference [37]. Copyright 2003, American Chemical Society.

which can further be enhanced by the subsequent overgrowth of the CS system with an additional ZnS shell.

5. Type-II and Reverse Type-I Systems

5.1. Synthesis of Type-II Core/Shell NCs

Research on colloidal type-II systems was triggered by the seminal work of Bawendi et al. who described the synthesis and optical properties of CdTe/CdSe and CdSe/ZnTe CS NCs.[37] The emission wavelength of CdTe/CdSe NCs could be tuned by changing the shell thickness and the core NC size from 700 to 1000 nm (Figure 9). This approach is an alternative possibility to shift the emission peak to higher wavelengths, which would not be attainable by simply increasing the size of the core NC in a type-I CS system. On the other hand, the observed mean decay lifetime (57 ns) was significantly larger than that of the corresponding core CdTe NCs (9.6 ns) and the QY was low (4%) with respect to type-I CS systems. CdTe/CdSe CS NCs were further synthesized without the use of organometallic precursors by applying CdO, TOPTe, and TOPSe. This approach lead to QYs approaching 40% for small shell thicknesses below 0.5 nm.[95] Chin et al. observed the formation of anisotropic (pyramids, multipods) structures during the overgrowth of spherical 2.6-nm CdTe NCs with CdSe using the SILAR technique (cf. §6).[96] CdSe/ZnTe NCs have been prepared with CdO as the cadmium precursor. Femtosecond dynamics measurements revealed that the rate of photoinduced electron/hole spatial separation decreased with increasing core size, while remaining independent of the shell thickness.[97]

ZnTe/CdTe represents the first common anion type-II system, reported by Basché et al.[98] The same article also includes the synthesis of ZnTe NCs with CdS and CdSe shells. These heterostructures were obtained by addition of precursors (cadmium oleate, TOPTe, TOPSe, or sulfur dissolved in octadecene) to the crude dispersion of ZnTe core NCs. QYs up to 30% have been observed, and the emission could be tuned in the range of 500–900 nm. Interestingly, the same group observed a transition from the concentric CS structure via pyramidal to tetrapod-shaped heterostructures in the case of the ZnTe/CdSe CS system, also described in Reference [99], when the shell growth was carried out at 215 °C instead of 240 °C (cf. Figure 10).[100] The CdS/ZnSe type-II system has been synthesized by adding zinc oleate and TOPSe to the CdS core NCs in a mixture of octadecylamine and ODE.[101] The obtained CS particles cover an emission range of 500–650 nm and a QY of 15%, which could be improved via the incorporation of cadmium in the shell.

5.2. Synthesis of Reverse Type-I Core/Shell NCs

Klimov and co-workers have studied the optical properties of so-called ''inverted'' CS NCs. These NCs are referred to as inverted due to the bandgap of their core material (ZnSe) being larger than that of their shell material (CdSe).[38] On the basis of the radiative recombination lifetimes recorded for NCs with a fixed core size and increasing shell thickness, a continuous transition from type I (both electron and hole wavefunctions are distributed over the entire NC) to type II (electron and hole are spatially separated between the shell and the core) and back to type I (both electron and hole primarily reside in the shell) localization regimes was observed. The samples exhibited emission in the range of 430–600 nm and QYs of 60–80%. The same CS system was also synthesized applying CdO dissolved with an excess of oleic acid in octadecene and TOPSe as the shell precursors, which were added very slowly over 2–3 hours.[15] By varying the CdSe shell thickness on 2.8-nm core ZnSe NCs, the emission wavelength could be tuned in a broad spectral range (417–678 nm) with QYs of 40–85% (Figure 11). Furthermore, size focusing during the shell growth has been observed, in

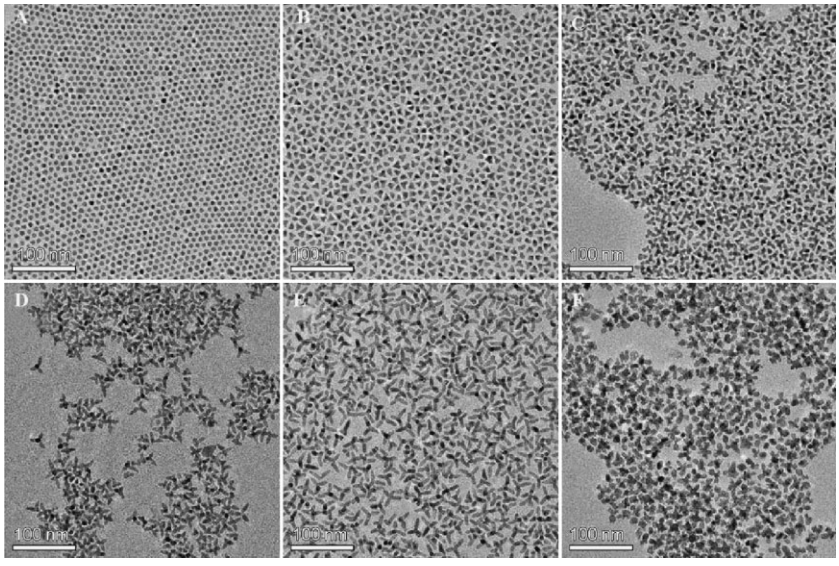

Figure 10. TEM images of ZnTe/CdSe NCs: transition from A) slightly anisotropic core/shell to B) pyramidal to C–D) tetrapod-shaped heterostructures with different arm lengths. F) TEM image of tetrapod-shaped ZnTe/CdS NCs. Reproduced with permission from Reference [100].

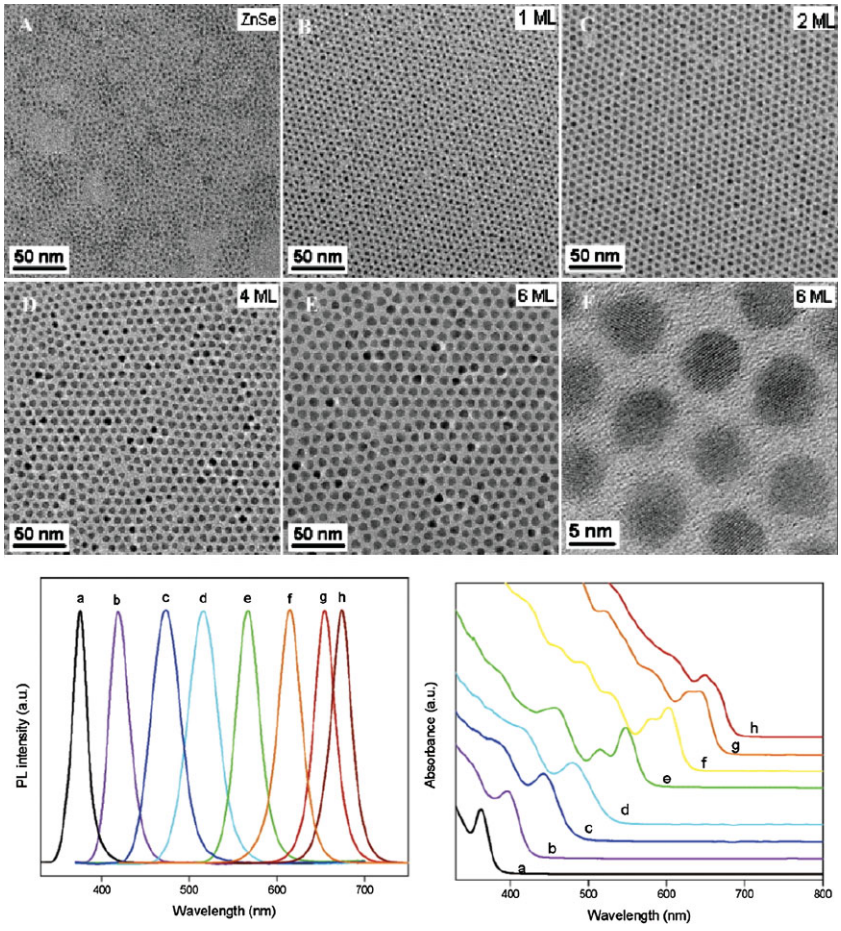

Figure 11. Top: TEM images of ZnSe core NCs and the corresponding ZnSe/CdSe core/shell NCs with different shell thicknesses (expressed in CdSe monolayers, ML). Bottom: Normalized PL (left) and corresponding absorption (right) spectra of ZnSe/CdSe CS NCs with different numbers of monolayers of CdSe shell: a) 0; b) 0.1; c) 0.2; d) 0.5; e) 1; f) 2; g) 4; h) 6. Reprinted with permission from Reference [15]. Copyright 2005, American Chemical Society.

contrast to the usually occurring broadening of the size distribution at this stage of the reaction.

NCs of a different inverted type-I system, namely, CdS/CdSe, were synthesized by Battaglia et al.[14] In this case, the emission wavelength could be varied from 520 to 650 nm by tuning the shell thickness. After growing a CdS shell on this system, the QY was improved from around 20% to 40%.

6. Core/Shell Systems of Anisotropic Shape

The shell growth on anisotropic NCs, such as nanorods or branched structures, bears additional difficulties with respect to spherical ones arising from the differences in reactivity of the different surface sites. Strain at the CS interface induced by the lattice mismatch of the core and the shell materials amplifies this problem and strongly impedes the homogeneous shell growth in such structures. The use of a graded CdS/ZnS shell on CdSe nanorods aiming at interfacial strain release has been described by Manna et al. This method allows for the variation of the shell thickness from 1–6 monolayers on core nanorods with aspect ratios ranging from 2:1 to 10:1.[102] In this context, the CdSe/CdS system deserves special attention, as here the growth of a 1D anisotropic (rodlike) shell on a 0D isotropic (spherical) core NCs has been achieved.[103] In the initial synthesis, CdS shell growth was carried out by the slow addition of organometallic Cd and S precursors (dimethylcadmium and $S(TMS)_2$). Crucial points for the anisotropic growth were the use of a relatively low reaction temperature of 130 °C and of an excess of the sulfur precursor (Cd/S = 1:3–1:5). The asymmetric shell growth has been rationalized by the different reactivity of the facets of the hexagonal CdSe core NCs and their different lattice mismatch with CdS. The obtained CS NCs exhibited linearly polarized emission with high QYs in the range of 70%, large Stokes shifts and a high molar-extinction coefficient ($10^7\,mol^{-1}\,cm^{-1}$ at 340 nm for NCs with an aspect ratio of 4:1).[103] The same system has further been optimized in the so-called "seeded growth" approach to an unprecedented level of control of length in the synthesis of anisotropic semiconductor NCs.[104] In particular, aspect ratios as high as 30:1 could be obtained via a new synthetic procedure, which relied on the rapid injection of CdSe seed NCs and elemental sulfur dissolved in TOP, into a solution of CdO in a mixture of TOPO, hexylphosphonic acid and octadecylphosphonic acid at high temperature (350–380 °C). The diameter of the studied rods varied between 3.5 and 5 nm, and the lengths ranged from 10–150 nm (Figure 12).

Due to their high degree of monodispersity, the nanorods could be self-assembled vertically on areas reaching several square micrometers. A similar route has been applied for the synthesis of another type of anisotropic heterostructure: CdSe/CdS tetrapods.[105] In this case, zinc blende CdSe seed NCs were injected together with sulfur into the cadmium precursor containing reaction mixture, leading to the growth of tetrapods containing a CdSe core and four CdS arms with lengths ranging from 15 to 46 nm, depending on the quantity of injected seeds.

Recently, multiple-branched NCs of CdTe/CdSe were synthesized from $Cd(Ac)_2$, octylphosphonic acid, TOPTe, and TOPSe in stearic acid and TOPO, and used in photovoltaic devices.[106] Chin et al. synthesized anisotropic CdTe/CdSe NCs, with shapes tunable from prolate-type I NCs to branched NCs exhibiting type-II character. The CdSe shell is grown by the dropwise and alternate addition of cadmium acetate in TOP and TOPSe at 150 °C, followed by 30 minutes of annealing at 130 °C. This synthesis method, at low temperature with slow precursor addition and low-reactivity precursors,

NANO MICRO small

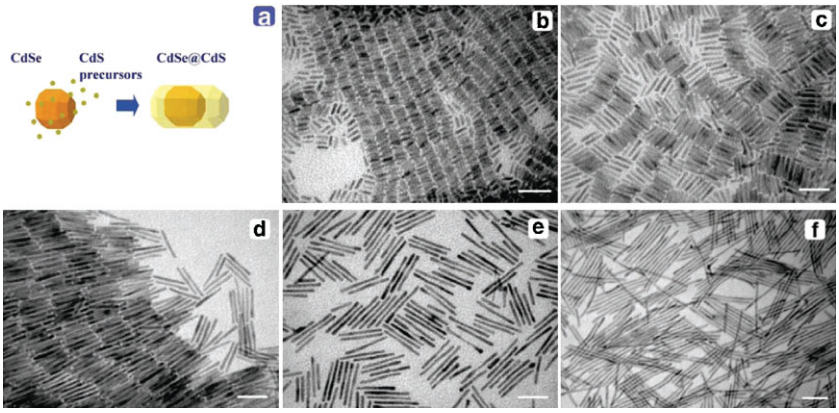

Figure 12. Self-assembly of CdSe/CdS nanorods prepared by the seeded-growth method, schematically depicted in (a). b–f) EM images of self-assembled CdSe/CdS nanorods. Small-aspect-ratio rods (b–d) tend to form locally ordered 2D smectic phases, while longer rods form either disordered assemblies, ribbons, or locally ordered 2D nematic phases. Average rod diameters and lengths, as determined by HRTEM, are: b) 4.9×19 nm; c) 4.2×35 nm; d) 3.9×53 nm; e) 3.8×70 nm; f) 3.8×111 nm. All scale bars are 50 nm long. Reprinted with permission from Reference [104]. Copyright 2007, American Chemical Society.

allows a slow and controlled growth of the CdSe shell leading to NCs with a high QY on the order of 80%.[96]

7. Core/Shell Systems Comprising Multiple Shells

7.1. Core/Shell/Shell Structures

One of the motivations for the synthesis of NCs containing multiple shells was the difficulty to respond simultaneously to the requirements of appropriate electronic (bandgap, band alignment) and structural (lattice mismatch) parameters for most binary CS systems. In particular the lattice mismatch between the core and the shell material strongly limits the possibility to grow a shell with significant thickness without deteriorating the photoluminescence properties. The use of a strain-reducing intermediate shell sandwiched between the core NC and an outer shell has first been proposed in the core/shell/shell (CSS) system CdSe/ZnSe/ZnS.[107,108] The energy-band alignment of this heterostructure corresponds to that depicted in the left panel of Figure 13. The interest of such structures lies in the combination of low strain, provided by the intermediate layer (ZnSe) serving as a "lattice adapter" and

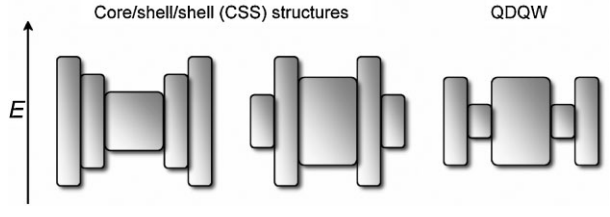

Figure 13. Schematic representation of the energy-level alignment in different CSS structures and in a QDQW system. The height of the rectangles represents the bandgap energy and their upper and lower edges correspond to the positions of the conduction- and valence-band edge, respectively, of the core (center) and shell materials.

efficient passivation and charge-carrier confinement assured by the outer shell (ZnS). The CSS system offers higher stability against photo-oxidation than the CS system of CdSe/ZnSe, and higher QYs than in the CS system of CdSe/ZnS, as evidenced by Talapin and co-workers who also extended this approach to CdSe/CdS/ZnS CSS NCs.[43] An aberration-corrected Z-contrast scanning transmission electron microscopy study of CdSe based CS NCs clearly revealed correlations between structure and QY.[109] Uniform shell coverage was observed only for graded shells (e.g., CdS/ZnS) and was found to be critical to achieving QYs close to unity. In this context, a multishell structure consisting of CdSe core $CdS/Zn_{0.5}Cd_{0.5}S/ZnS$ has been synthesized using the SILAR technique.[110] The monodisperse samples obtained in this study exhibit QYs of 70–85% and enhanced stability as compared to their binary CS counterparts. The same arguments apply for InAsP/InP/ZnSe NCs, a near-infrared-emitting III–V-semiconductor-based CSS heterostructure.[111] In another approach, InAs NCs were overcoated with a CdSe/ZnSe double shell, exhibiting high QYs up to 70% in the spectral region of 800–1600 nm.[112]

As mentioned before, the QYs of type-II CS systems are comparably low, and a limiting factor is the fact that one of the charge carriers is located in the shell material, only passivated by organic surfactant molecules. A logical step consists, therefore, in the addition of a large-bandgap outer layer, resulting in a CSS system. Such a heterostructure has been realized by the synthesis of CdSe/ZnTe/ZnS NCs.[113] A different type of band alignment has been achieved in CdSe/CdTe/ZnTe. Here, the intermediate CdTe shell serves as a barrier layer for electrons (CdSe) and holes (ZnTe), resulting in a strongly increased radiative lifetime, estimated as 10 ms.[97]

7.2. Quantum Dot/Quantum Wells and Inverse Structures

Quantum-dot quantum-well (QDQW) structures represent the special case of a CSS structure in which a lower-bandgap layer is embedded between a higher-bandgap core and outer shell material with both semiconductors having type-I band alignment (cf. right panel in Figure 13). Among the first systems studied was CdS/HgS/CdS.[114] Due to the different solubility parameters of CdS and HgS in aqueous solution, the outermost monolayer of CdS NCs can be selectively substituted with HgS by addition of mercury perchlorate. In the following, the released Cd ions are re-deposited on the CdS/HgS NCs in form of CdS, induced by H_2S addition. This system has more recently been extended to heterostructures comprising two embedded HgS layers.[115,116] Other systems studied comprise ZnS/CdS/ZnS,[117] and CdS/CdSe/CdS,[25] which were prepared using the SILAR technique. This method is particularly well adapted for the

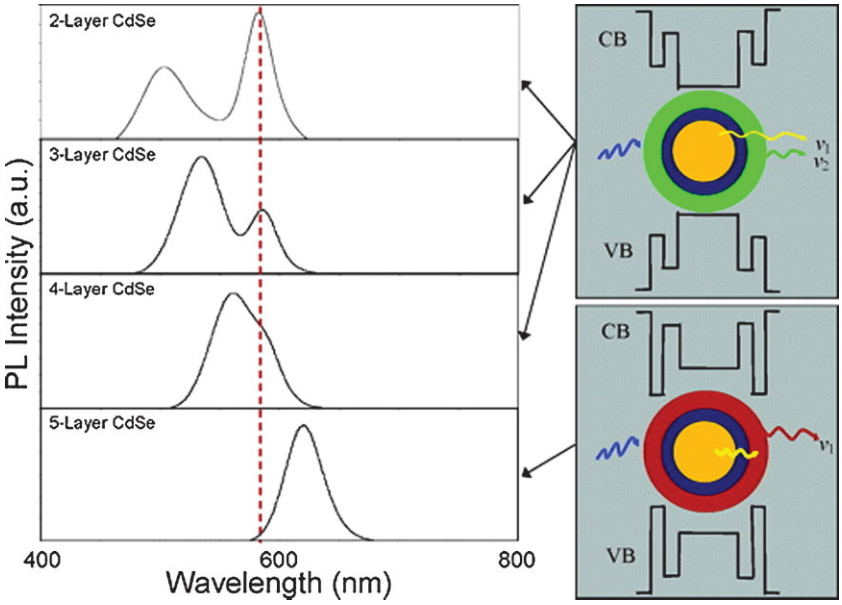

Figure 14. CdSe/ZnS/CdSe CSS NCs. Left: PL spectra as a function of the outer CdSe shell thickness. Right: Corresponding energy-band structures and schemes displaying the different absorption and emission processes. Reprinted with permission from Reference [120]. Copyright 2005, American Chemical Society.

fabrication of QDQW structures due to the precise control of the shell thickness. The latter system has also been modeled by large-scale pseudopotential local density approximation (LDA) calculations,[118] indicating that the conduction-band wavefunction is less confined to the CdSe well layer than predicted by effective-mass theory.[119]

An "inverse" QDQW structure has been realized with the synthesis of CdSe/ZnS/CdSe NCs, as here the larger-bandgap material is embedded between the lower-bandgap ones (middle panel in Figure 13).[120] This heterostructure represents the first structure simultaneously exhibiting two distinct emission wavelengths coming from both the CdSe core and the outer shell (Figure 14), a phenomenon that has subsequently been used for the generation of white light.[121] In order to have electronic decoupling of the CdSe core and outer shell, the ZnS intermediate shell must have a minimum thickness of around three monolayers.[120] Further photophysical studies concerning the energy transfer between the CdSe core and outer shell have recently been carried out on this system.[122]

8. Summary and Outlook

In view of the developments in the domain of CS semiconductor NCs in the past decade, it can be speculated that a large variety of new heterostructures with exciting and, in some cases, unprecedented features will be synthesized by chemical routes in the next few years. The ability to precisely control the shell thickness will further boost advances in the preparation of nonblinking NCs, CSS, and other complex structures such as QDQWs. Significant progress has been achieved in the field of anisotropic shell growth on spherical CdSe NCs, leading to new rod-shaped CS nanostructures, which combine unique optical properties (high QY, polarized emission) with appealing self-assembly properties. The developed synthesis method using small-core NCs as seeds in the so-called seeded-growth approach[104,105] opens up the way for a generation of new heterostructures, including nanorods and branched structures such as bi-, tri-, tetra- or multipods.

Similar to the case of II–VI compounds, it can be expected that a growing number of CS systems based on III–V semiconductors will be developed, inspired by the huge amount of research carried out in the field of III–V nanostructures grown by molecular-beam epitaxy (MBE) techniques. On the one hand, the growth of such new CS systems with high-quality optical properties provides intriguing motivation for fundamental research. On the other hand, the use of alternative core materials is mandatory for most commercial applications, in view of the low acceptability of cadmium, lead, mercury, or arsenide-containing compounds. Ternary semiconductors such as chalcopyrites or doped NCs (e.g., ZnSe:Mn) may gain importance in this context. A better understanding of the involved reaction mechanisms, side reactions and NCs' surface chemistry is indispensable for the rational design of synthesis strategies for new CS systems. Efforts in this direction have recently been undertaken in the case of CdSe and PbSe core NCs.[123,124]

Finally, the association of semiconductors with other materials such as metals or oxides in the same CS heterostructure allows for the design of NCs combining different physical properties, for example, fluorescence, magnetism, different decay lifetimes, and so on.[8] In such a manner, novel functional building blocks can be generated for applications in fields ranging from optoelectronics to information technology to healthcare. In most of these examples, the CS NCs are used as a platform for further surface functionalization, providing the ability to tune their assembly properties on given substrates or their solubility in various media, or to induce their binding to other molecules or macromolecules.

Acknowledgements

Financial support from CEA (program "Technologies pour la Santé", project TIMOMA2) and from ANR (project SYNERGIE) are acknowledged. Cydnie Bedford and Andreu Cabot are thanked for critical review of the manuscript.

Keywords:

core/shell materials · nanocrystals · photoluminescence · quantum dots · semiconductors

[1] M. A. Hines, P. Guyot-Sionnest, *J. Phys. Chem.* **1996**, *100*, 468–471.

[2] B. O. Dabbousi, J. RodriguezViejo, F. V. Mikulec, J. R. Heine, H. Mattoussi, R. Ober, K. F. Jensen, M. G. Bawendi, *J. Phys. Chem. B* **1997**, *101*, 9463–9475.
[3] X. G. Peng, M. C. Schlamp, A. V. Kadavanich, A. P. Alivisatos, *J. Am. Chem. Soc.* **1997**, *119*, 7019–7029.
[4] D. Dorfs, A. Eychmüller, *Z. Phys. Chem.* **2006**, *220*, 1539–1552.
[5] J. Van Emden, J. Jasieniak, D. E. Gomez, P. Mulvaney, M. Giersig, *Aust. J. Chem.* **2007**, *60*, 457–471.
[6] G. D. Scholes, *Adv. Funct. Mater.* **2008**, *18*, 1157–1172.
[7] J. Park, J. Joo, S. G. Kwon, Y. Jang, T. Hyeon, *Angew. Chem. Int. Ed.* **2007**, *46*, 4630–4660.
[8] P. D. Cozzoli, T. Pellegrino, L. Manna, *Chem. Soc. Rev.* **2006**, *35*, 1195–1208.
[9] I. L. Medintz, H. T. Uyeda, E. R. Goldman, H. Mattoussi, *Nat. Mater.* **2005** *4*, 435–446.
[10] T. Pellegrino, S. Kudera, T. Liedl, A. M. Javier, L. Manna, W. J. Parak, *Small* **2005**, *1*, 48–63.
[11] J. M. Klostranec, W. C. W. Chan, *Adv. Mater.* **2006**, *18*, 1953–1964.
[12] S. H. Wei, A. Zunger, *Appl. Phys. Lett.* **1998**, *72*, 2011–2013.
[13] A. Mews, A. Eychmüller, M. Giersig, D. Schooss, H. Weller, *J. Phys. Chem.* **1994**, *98*, 934–941.
[14] D. Battaglia, J. J. Li, Y. J. Wang, X. G. Peng, *Angew. Chem. Int. Ed.* **2003**, *42*, 5035–5039.
[15] X. H. Zhong, R. G. Xie, Y. Zhang, T. Basché, W. Knoll, *Chem. Mater.* **2005**, *17*, 4038–4042.
[16] P. Sarkar, M. Springborg, G. Seifert, *Chem. Phys. Lett.* **2005**, *405*, 103–107.
[17] J. B. Li, L. W. Wang, *Appl. Phys. Lett.* **2004**, *84*, 3648–3650.
[18] A. Piryatinski, S. A. Ivanov, S. Tretiak, V. I. Klimov, *Nano Lett.* **2007**, *7*, 108–115.
[19] X. B. Chen, Y. B. Lou, A. C. Samia, C. Burda, *Nano Lett.* **2003**, *3*, 799–803.
[20] O. Madelung, M. Schulz, H. Weiss, *Numerical Data and Functional Relationships in Science and Technology, New Series, Group III: Crystal and Solid State Physics, Vol. vol. III/17b*, Springer, Berlin **1982**.
[21] J. Singh, *Physics of Semiconductors and Their Heterostructures*, McGraw-Hill, New York **1993**.
[22] W. W. Yu, L. H. Qu, W. Z. Guo, X. G. Peng, *Chem. Mater.* **2003**, *15*, 2854–2860.
[23] S. Adam, D. V. Talapin, H. Borchert, A. Lobo, C. McGinley, A. R. B. de Castro, M. Haase, H. Weller, T. Moller, *J. Chem. Phys.* **2005**, *123*.
[24] D. V. Talapin, PhD thesis, Hamburg **2002**.
[25] J. J. Li, Y. A. Wang, W. Z. Guo, J. C. Keay, T. D. Mishima, M. B. Johnson, X. G. Peng, *J. Am. Chem. Soc.* **2003**, *125*, 12567–12575.
[26] W. K. Bae, K. Char, H. Hur, S. Lee, *Chem. Mater.* **2008**, *20*, 531–539.
[27] Z. H. Yu, L. Guo, H. Du, T. Krauss, J. Silcox, *Nano Lett.* **2005**, *5*, 565–570.
[28] H. Borchert, D. V. Talapin, C. McGinley, S. Adam, A. Lobo, A. R. B. de Castro, T. Moller, H. Weller, *J. Chem. Phys.* **2003**, *119*, 1800–1807.
[29] H. Borchert, S. Haubold, M. Haase, H. Weller, *Nano Lett.* **2002**, *2*, 151–154.
[30] J. N. Gillet, M. Meunier, *J. Phys. Chem. B* **2005**, *109*, 8733–8737.
[31] J. E. B. Katari, V. L. Colvin, A. P. Alivisatos, *J. Phys. Chem.* **1994**, *98*, 4109–4117.
[32] A. Eychmüller, *J. Phys. Chem. B* **2000**, *104*, 6514–6528.
[33] G. Rafeletos, S. Norager, P. O'Brien, *J. Mater. Chem.* **2001**, *11*, 2542–2544.
[34] A. V. Baranov, Y. P. Rakovich, J. F. Donegan, T. S. Perova, R. A. Moore, D. V. Talapin, A. L. Rogach, Y. Masumoto, I. Nabiev, *Physical Review B* **2003**, *68*.
[35] A. Singha, B. Satpati, P. V. Satyam, A. Roy, *J. Phys. Cond. Matt.* **2005**, *17*, 5697–5708.
[36] F. S. Manciu, R. E. Tallman, B. D. McCombe, B. A. Weinstein, D. W. Lucey, Y. Sahoo, P. N. Prasad, *Physica E* **2005**, *26*, 14–18.
[37] S. Kim, B. Fisher, H. J. Eisler, M. Bawendi, *J. Am. Chem. Soc.* **2003**, *125*, 11466–11467.
[38] L. P. Balet, S. A. Ivanov, A. Piryatinski, M. Achermann, V. I. Klimov, *Nano Lett.* **2004**, *4*, 1485–1488.
[39] T. Mokari, U. Banin, *Chem. Mater.* **2003**, *15*, 3955–3960.
[40] D. V. Talapin, A. L. Rogach, A. Kornowski, M. Haase, H. Weller, *Nano Lett.* **2001**, *1*, 207–211.
[41] S. Kudera, M. Zanella, C. Giannini, A. Rizzo, Y. Q. Li, G. Gigli, R. Cingolani, G. Ciccarella, W. Spahl, W. J. Parak, L. Manna, *Adv. Mater.* **2007**, *19*, 548–551.
[42] S. Jun, E. Jang, *Chem. Commun.* **2005**, 4616–4618.
[43] D. V. Talapin, I. Mekis, S. Gotzinger, A. Kornowski, O. Benson, H. Weller, *J. Phys. Chem. B* **2004**, *108*, 18826–18831.
[44] S. J. Lim, B. Chon, T. Joo, S. K. Shin, *J. Phys. Chem. C* **2008**, *112*, 1744–1747.
[45] S. Wang, B. R. Jarrett, S. M. Kauzlarich, A. Y. Louie, *J. Am. Chem. Soc.* **2007**, *129*, 3848–3856.
[46] Y. Chen, J. Vela, H. Htoon, J. L. Casson, D. J. Werder, D. A. Bussian, V. I. Klimov, J. A. Hollingsworth, *J. Am. Chem. Soc.* **2008**, *130*, 5026–5027.
[47] B. Mahler, P. Spinicelli, S. Buil, X. Quelin, J. P. Hermier, B. Dubertret, *Nat. Mater.* **2008** *7*, 659–664.
[48] M. A. Malik, P. O'Brien, N. Revaprasadu, *Chem. Mater.* **2002**, *14*, 2004–2010.
[49] N. Revaprasadu, M. A. Malik, P. O'Brien, G. Wakefield, *Chem. Commun.* **1999**, 1573–1574.
[50] I. Mekis, D. V. Talapin, A. Kornowski, M. Haase, H. Weller, *ccc B* **2003**, *107*, 7454–7462.
[51] D. C. Pan, Q. Wang, S. C. Jiang, X. L. Ji, L. J. An, *Adv. Mater.* **2005**, *17*, 176–178.
[52] S. Asokan, K. M. Krueger, A. Alkhawaldeh, A. R. Carreon, Z. Z. Mu, V. L. Colvin, N. V. Mantzaris, M. S. Wong, *Nanotechnology* **2005**, *16*, 2000–2011.
[53] Y. W. Lin, M. M. Hsieh, C. P. Liu, H. T. Chang, *Langmuir* **2005**, *21*, 728–734.
[54] M. Danek, K. F. Jensen, C. B. Murray, M. G. Bawendi, *Chem. Mater.* **1996**, *8*, 173–180.
[55] P. Reiss, J. Bleuse, A. Pron, *Nano Lett.* **2002**, *2*, 781–784.
[56] P. Reiss, S. Carayon, J. Bleuse, *Physica E* **2003**, *17*, 95–96.
[57] Y. J. Lee, T. G. Kim, Y. M. Sung, *Nanotechnology* **2006**, *17*, 3539–3542.
[58] Y. M. Sung, K. S. Park, Y. J. Lee, T. G. Kim, *J. Phys. Chem. C* **2007**, *111*, 1239–1242.
[59] J. S. Steckel, P. Snee, S. Coe-Sullivan, J. R. Zimmer, J. E. Halpert, P. Anikeeva, L. A. Kim, V. Bulovic, M. G. Bawendi, *Angew. Chem. Int. Ed.* **2006**, *45*, 5796–5799.
[60] M. Protiere, P. Reiss, *Small* **2007**, *3*, 399–403.
[61] L. Spanhel, M. Haase, H. Weller, A. Henglein, *J. Am. Chem. Soc.* **1987**, *109*, 5649–5655.
[62] J. S. Steckel, J. P. Zimmer, S. Coe-Sullivan, N. E. Stott, V. Bulovic, M. G. Bawendi, *Angew. Chem. Int. Ed.* **2004**, *43*, 2154–2158.
[63] M. Protiere, P. Reiss, *Nanoscale Res. Lett.* **2006**, *1*, 62–67.
[64] Y. A. Yang, O. Chen, A. Angerhofer, Y. C. Cao, *J. Am. Chem. Soc.* **2006**, *128*, 12428–12429.
[65] H. Yang, P. H. Holloway, *Adv. Funct. Mater.* **2004**, *14*, 152–156.
[66] M. Lomascolo, A. Creti, G. Leo, L. Vasanelli, L. Manna, *Appl. Phys. Lett.* **2003**, *82*, 418–420.
[67] H. S. Chen, B. Lo, J. Y. Hwang, G. Y. Chang, C. M. Chen, S. J. Tasi, S. J. J. Wang, *J. Phys. Chem. B* **2004**, *108*, 17119–17123.
[68] J. M. Tsay, M. Pflughoefft, L. A. Bentolila, S. Weiss, *J. Am. Chem. Soc.* **2004**, *126*, 1926–1927.
[69] A. L. Rogach, T. Franzl, T. A. Klar, J. Feldmann, N. Gaponik, V. Lesnyak, A. Shavel, A. Eychmüller, Y. P. Rakovich, J. F. Donegan, *J. Phys. Chem. C* **2007**, *111*, 14628–14637.

[70] H. B. Bao, Y. J. Gong, Z. Li, M. Y. Gao, *Chem. Mater.* **2004**, *16*, 3853–3859.
[71] Y. He, H. T. Lu, L. M. Sai, W. Y. Lai, Q. L. Fan, L. H. Wang, W. Huang, *J. Phys. Chem. B* **2006**, *110*, 13370–13374.
[72] C. L. Wang, H. Zhang, J. H. Zhang, M. J. Li, H. Z. Sun, B. Yang, *Journal of Physical Chemistry C* **2007**, *111*, 2465–2469.
[73] M. T. Harrison, S. V. Kershaw, A. L. Rogach, A. Kornowski, A. Eychmüller, H. Weller, *Adv. Mater.* **2000**, *12*, 123–125.
[74] O. I. Mićić, H. M. Cheong, H. Fu, A. Zunger, J. R. Sprague, A. Mascarenhas, A. J. Nozik, *J. Phys. Chem. B* **1997**, *101*, 4904–4912.
[75] O. I. Mićić, C. J. Curtis, K. M. Jones, J. R. Sprague, A. J. Nozik, *J. Phys. Chem.* **1994**, *98*, 4966–4969.
[76] A. A. Guzelian, J. E. B. Katari, A. V. Kadavanich, U. Banin, K. Hamad, E. Juban, A. P. Alivisatos, R. H. Wolters, C. C. Arnold, J. R. Heath, *J. Phys. Chem.* **1996**, *100*, 7212–7219.
[77] D. V. Talapin, N. Gaponik, H. Borchert, A. L. Rogach, M. Haase, H. Weller, *J. Phys. Chem. B* **2002**, *106*, 12659–12663.
[78] O. I. Mićić, J. Sprague, Z. H. Lu, A. J. Nozik, *Appl. Phys. Lett.* **1996**, *68*, 3150–3152.
[79] S. Haubold, M. Haase, A. Kornowski, H. Weller, *ChemPhysChem* **2001**, *2*, 331–334.
[80] O. I. Mićić, B. B. Smith, A. J. Nozik, *J. Phys. Chem. B* **2000**, *104*, 12149–12156.
[81] S. Xu, J. Ziegler, T. Nann, *J. Mater. Chem.* **2008**, *18*, 2653–2656.
[82] R. Xie, D. Battaglia, X. Peng, *J. Am. Chem. Soc.* **2007**, *129*, 15432–15433.
[83] L. Li, M. Protière, P. Reiss, *Chem. Mater.* **2008**, *20*, 2621–2623.
[84] L. Li, P. Reiss, *J. Am. Chem. Soc.* **2008**, *130*, 11588–11589.
[85] Y. W. Cao, U. Banin, *Angew. Chem. Int. Ed.* **1999**, *38*, 3692–3694.
[86] Y. W. Cao, U. Banin, *J. Am. Chem. Soc.* **2000**, *122*, 9692– 9702.
[87] J. P. Zimmer, S. W. Kim, S. Ohnishi, E. Tanaka, J. V. Frangioni, M. G. Bawendi, *J. Am. Chem. Soc.* **2006**, *128*, 2526–2527.
[88] M. Brumer, A. Kigel, L. Amirav, A. Sashchiuk, O. Solomesch, N. Tessler, E. Lifshitz, *Adv. Funct. Mater.* **2005**, *15*, 1111–1116.
[89] E. Lifshitz, M. Brumer, A. Kigel, A. Sashchiuk, M. Bashouti, M. Sirota, E. Galun, Z. Burshtein, A. Q. Le Quang, I. Ledoux–Rak, J. Zyss, *J. Phys. Chem. B* **2006**, *110*, 25356–25365.
[90] A. Sashchiuk, L. Langof, R. Chaim, E. Lifshitz, *J. Cryst. Growth* **2002**, *240*, 431–438.
[91] J. Xu, D. H. Cui, T. Zhu, G. Paradee, Z. Q. Liang, Q. Wang, S. Y. Xu, A. Y. Wang, *Nanotechnology* **2006**, *17*, 5428–5434.
[92] D. V. Talapin, H. Yu, E. V. Shevchenko, A. Lobo, C. B. Murray, *J. Phys. Chem. C* **2007**, *111*, 14049–14054.
[93] J. W. Stouwdam, J. Shan, F. van Veggel, A. G. Pattantyus–Abraham, J. F. Young, M. Raudsepp, *J. Phys. Chem. C* **2007**, *111*, 1086–1092.
[94] J. M. Pietryga, D. J. Werder, D. J. Williams, J. L. Casson, R. D. Schaller, V. I. Klimov, J. A. Hollingsworth, *J. Am. Chem. Soc.* **2008**, *130*, 4879–4885.
[95] K. Yu, B. Zaman, S. Romanova, D. S. Wang, J. A. Ripmeester, *Small* **2005**, *1*, 332–338.
[96] P. T. K. Chin, C. D. M. Donega, S. S. Bavel, S. C. J. Meskers, N. Sommerdijk, R. A. J. Janssen, *J. Am. Chem. Soc.* **2007**, *129*, 14880–14886.
[97] C. Y. Chen, C. T. Cheng, C. W. Lai, Y. H. Hu, P. T. Chou, Y. H. Chou, H. T. Chiu, *Small* **2005**, *1*, 1215–1220.
[98] R. G. Xie, X. H. Zhong, T. Basché, *Adv. Mater.* **2005**, *17*, 2741–2744.
[99] D. J. Milliron, S. M. Hughes, Y. Cui, L. Manna, J. B. Li, L. W. Wang, A. P. Alivisatos, *Nature* **2004**, *430*, 190–195.
[100] R. G. Xie, U. Kolb, T. Basché, *Small* **2006**, *2*, 1454–1457.
[101] S. A. Ivanov, A. Piryatinski, J. Nanda, S. Tretiak, K. R. Zavadil, W. O. Wallace, D. Werder, V. I. Klimov, *J. Am. Chem. Soc.* **2007**, *129*, 11708–11719.
[102] L. Manna, E. C. Scher, L. S. Li, A. P. Alivisatos, *J. Am. Chem. Soc.* **2002**, *124*, 7136–7145.
[103] D. V. Talapin, R. Koeppe, S. Gotzinger, A. Kornowski, J. M. Lupton, A. L. Rogach, O. Benson, J. Feldmann, H. Weller, *Nano Lett.* **2003**, *3*, 1677–1681.
[104] L. Carbone, C. Nobile, M. De Giorg, F. D. Sala, G. Morello, P. Pompa, M. Hytch, E. Snoeck, A. Fiore, I. R. Franchini, M. Nadasan, A. F. Silvestre, L. Chiodo, S. Kudera, R. Cingolani, R. Krahne, L. Manna, *Nano Lett.* **2007**, *7*, 2942–2950.
[105] D. V. Talapin, J. H. Nelson, E. V. Shevchenko, S. Aloni, B. Sadtler, A. P. Alivisatos, *Nano Lett.* **2007**, *7*, 2951–2959.
[106] H. Z. Zhong, Y. Zhou, Y. Yang, C. H. Yang, Y. F. Li, *J. Phys. Chem. C* **2007**, *111*, 6538–6543.
[107] J. Bleuse, S. Carayon, P. Reiss, *Physica E* **2004**, *21*, 331–335.
[108] P. Reiss, S. Carayon, J. Bleuse, A. Pron, *Synth. Met.* **2003**, *139*, 649–652.
[109] J. McBride, J. Treadway, L. C. Feldman, S. J. Pennycook, S. J. Rosenthal, *Nano Lett.* **2006**, *6*, 1496–1501.
[110] R. G. Xie, U. Kolb, J. X. Li, T. Basché, A. Mews, *J. Am. Chem. Soc.* **2005**, *127*, 7480–7488.
[111] S. W. Kim, J. P. Zimmer, S. Ohnishi, J. B. Tracy, J. V. Frangioni, M. G. Bawendi, *J. Am. Chem. Soc.* **2005**, *127*, 10526–10532.
[112] A. Aharoni, T. Mokari, I. Popov, U. Banin, *J. Am. Chem. Soc.* **2006**, *128*, 257–264.
[113] C. T. Cheng, C. Y. Chen, C. W. Lai, W. H. Liu, S. C. Pu, P. T. Chou, Y. H. Chou, H. T. Chiu, *J. Mater. Chem.* **2005**, *15*, 3409–3414.
[114] A. Eychmüller, A. Mews, H. Weller, *Chem. Phys. Lett.* **1993**, *208*, 59–62.
[115] M. Braun, C. Burda, M. A. El–Sayed, *J. Phys. Chem. A* **2001**, *105*, 5548–5551.
[116] H. Borchert, D. Dorfs, C. McGinley, S. Adam, T. Moller, H. Weller, A. Eychmüller, *J. Phys. Chem. B* **2003**, *107*, 7486–7491.
[117] R. B. Little, M. A. El–Sayed, G. W. Bryant, S. Burke, *J. Chem. Phys.* **2001**, *114*, 1813–1822.
[118] J. Schrier, L. W. Wang, *Phys. Rev. B* **2006**, *73*.
[119] T. Stirner, *J. Chem. Phys.* **2002**, *117*, 6715–6720.
[120] D. Battaglia, B. Blackman, X. G. Peng, *J. Am. Chem. Soc.* **2005**, *127*, 10889–10897.
[121] S. Sapra, S. Mayilo, T. A. Klar, A. L. Rogach, J. Feldmann, *Adv. Mater.* **2007**, *19*, 569–571.
[122] E. A. Dias, S. L. Sewall, P. Kambhampati, *J. Phys. Chem. C* **2007**, *111*, 708–713.
[123] H. T. Liu, J. S. Owen, A. P. Alivisatos, *J. Am. Chem. Soc.* **2007**, *129*, 305–312.
[124] J. S. Steckel, B. K. H. Yen, D. C. Oertel, M. G. Bawendi, *J. Am. Chem. Soc.* **2006**, *128*, 13032–13033.

Received: June 12, 2008